Proceedings of the Sixth International Conference on
Railway Technology: Research, Development and Maintenance
Edited by: J. Pombo
Civil-Comp Conferences, Volume 7, Paper 22.1
Civil-Comp Press, Edinburgh, United Kingdom, 2024
ISSN: 2753-3239, doi: 10.4203/ccc.7.22.1
©Civil-Comp Ltd, Edinburgh, UK, 2024

Study on the Significant Influencing Factors on Vehicle Operational Stability in Large-Size Turnout Areas

Y. Li[1,2,3], Y. Qian[1,3], Z. Liu[1,3], J. Xu[1,3], R. Chen[1,3] and Y. Luo[1,3]

[1]School of Civil Engineering, Southwest Jiaotong University
Chengdu, China
[2]School of Civil Engineering, Lanzhou Jiaotong University
Lanzhou, China
[3]Key Laboratory of High-Speed Railway Engineering,Ministry of Education, Southwest Jiaotong University, Chengdu, China

Abstract

At present, there are many cases of lateral vibration acceleration exceeding the limit when a high-speed vehicle passes the large-size turnout in the diverging route, which affects the smoothness of vehicle operation and the comfort of passengers. Therefore, this paper proposes a vehicle-turnout coupled dynamic model considering both rigid and flexible characteristics. By utilizing orthogonal experiments and the Plackett-Burman saturated fractional factorial design method, the lateral vibration acceleration of the vehicle body and the Sperling lateral stability index are selected as the observed variables. Employing the graphical analysis method, significant influential factors affecting the vehicle operational stability of high-speed vehicle passes large-size turnout in the diverging route are identified. The results show that: 1) The driving speed has a pronounced influence on various aspects, including lateral wheel-rail forces, bogie vibration acceleration, lateral vibration acceleration of the vehicle body, and the lateral Sperling stability index; 2) The wheel profile exerts a significant impact on the lateral wheel-rail forces and the lateral vibration acceleration of the bogie. However, its influence on the lateral vibration acceleration of the vehicle body and the lateral Sperling stability index is relatively negligible; 3) The influence of rail profile on frame transverse vibration acceleration and body transverse vibration acceleration is more obvious. Under the rail abrasion condition, the frame transverse vibration acceleration increased by 69.36% compared with the standard profile, and the maximum value of body transverse vibration acceleration increased by 31.87% compared with the standard profile.

Keywords: vehicle operational stability, driving speed, wheel profile, rail profile, Significant Factor Selection

1 Introduction

At present, there is a significant occurrence of lateral oscillations, commonly known as "carbody's hunting", when high-speed trains pass large-size turnout in the diverging route on China's passenger dedicated line equipped with 60kg/m rail. This phenomenon has a considerable impact on the operational stability of the trains and the overall comfort experienced by passengers. Throughout the operational phase, remedial efforts have primarily relied on controlling geometric dimensions, yet the observed outcomes have not yielded substantial improvements. Hence, a comprehensive investigation is warranted to thoroughly examine the significant factors influencing vehicle operational stability in large-size turnout areas.

In the study on vehicle stability conducted by O. Polach [1], a comparison was made between two different nonlinear stability criteria. The findings revealed that under nonlinear conditions, the critical values not only depend on the calculation methods but also on the wheel-rail compatibility. N. Wilson [2] conducted a scholarly investigation employing vehicle experiments, wheel-rail profile measurements, and NUCARS simulations. The study concluded that suspension parameters, vehicle body inertia parameters, and wheel-rail compatibility conditions have a significant impact on the lateral stability of the vehicle. Xusheng He [3]et al. conducted a scholarly investigation that involved testing the vibration characteristics of high-speed trains under operating conditions, with a specific focus on the wheel tread profile. The researchers analyzed the equivalent conicity of the wheel and investigated the relationship between wheel-rail compatibility and carbody's hunting phenomenon. Maoru Chi [4] et al conducted a scholarly analysis focusing on the vibration modes of the vehicle's bogie and body. The study identified that when the lateral oscillation frequency of the bogie approaches the natural frequency of the vehicle body, resonance occurs, thereby significantly impacting the vehicle's stability during operation. Shanchao Sun [5]et al.employed multibody dynamics software to construct a dynamic model of a high-speed monitoring vehicle. The study focused on analyzing the impact of wheel-rail compatibility on the vibration characteristics of the vehicle's bogie. Additionally, the researchers investigated the mechanisms by which these factors influence the vehicle's operational stability. Wenli Yang [6]et al conducted a scholarly investigation wherein they analyzed the impact of various track irregularities on the operational stability of vehicles. This was achieved through the detection of prominent track irregularities along the main line and the measurement of vehicle body vibration acceleration. Zhichao Zhang [7] et al conducted a scholarly investigation focusing on the correlation between carbody's hunting phenomenon and factors such as the equivalent conicity of the wheel-rail system and the installation angle of anti-hunting motion dampers. They developed a dynamic simulation model to study the problem of lateral instability in the vehicle's body. Litong Cui [8] et al. proposed that the fundamental cause of carbody's hunting phenomenon is attributed to poor quality of wheel-rail profiling, which results in a deteriorated wheel-rail compatibility, rather than being caused by track irregularities or cant deficiencies.

Shuguo Wang [9]et al conducted a scholarly investigation pertaining to the stability of train passage over 42# turnout. They specifically studied the impact of switch rail on the longitudinal stability during turnout crossing. The study emphasized that when the switch rail value exceeds the specified limits, it leads to a decrease in the stability when the vehicle rolls across the turnout. Jun Jiang [10] et al conducted a scholarly analysis that comprehensively examined the influence of factors such as track excitation, wheel-rail geometric compatibility, and environmental conditions on the longitudinal stability of high-speed trains during turnout crossings. Their study contributes to the theoretical basis for enhancing the stability when the vehicle rolls across the turnout. Ping Wang [11] et al proposed a method to improve the operational stability when the vehicle rolls across the turnout by optimizing the cross-section of the point rail in high-speed railway turnouts. The study focuses on enhancing the design of the point rail section to minimize vibrations and ensure smoother train movement during turnout crossings. Wang Yonghua [12] conducted a scholarly investigation focusing on the issue of inertial oscillation points in the northern turnout area of the Bengbu South Station on the Beijing-Shanghai High-Speed Railway. Taking this case as an example, the study proposed that research and maintenance of the rail profile, specifically through grinding techniques, play a critical role in addressing the problem of inertial oscillation points in turnouts.

2 Vehicle-turnout rigid-flexible coupling dynamic model and simulation analysis

In order to delve into the factors influencing the lateral stability of the vehicle passes large-size turnout in the diverging route, this study takes into account the computational accuracy and efficiency of the model. Based on the CRH380A train and 42# turnout, through the integration of finite element software and multibody dynamics software, a rigorous and flexible coupling dynamic model of the vehicle-turnout system is established. The developed dynamic simulation model is employed to analyze the wheel-rail interactions during the high-speed vehicle passes 42# turnout in the diverging route of the facing move and trailing move, thereby assessing vehicle operational stability.

2.1 Vehicle-turnout rigid-flexible coupling dynamic model

This paper presents the development of a high-speed railway vehicle dynamic model based on the CRH380A prototype. The model comprises various components, including the carbody, bogie, axle box, and wheelset, forming a multibody system. During the modeling process, all the components are idealized as rigid bodies to facilitate analysis. Specifically, the carbody, bogie, and wheelset possess six degrees of freedom each, allowing for a comprehensive representation of their motion characteristics. On the other hand, the axle box is characterized by only one degree of freedom, considering its predominantly vertical motion. For detailed calculation parameters of the vehicle model, please refer to the relevant literature [13].

Taking No.42 turnout as a prototype, In ABAQUS, a finite element model of a turnout track is established by employing Timoshenko beam elements. The turnout

components, namely the steel rails, are simplified as beam models. The model includes six distinct beams: the straight stock rail, curved stock rail, straight switch rail (consisting of the switch rail, connecting portion, and left wing rail), curved switch rail (comprising the switch rail, connecting portion, and right wing rail), long guard rail, and short guard rail. In order to account for the impact of transition sections before and after the turnout, 30 m long interval tracks are introduced at both ends, resulting in a total model length of 217.2 m. Each beam element has a length of 0.15 m, and there are four beam elements per sleeper span. To model the under-rail support, constraints, and interactions between the steel rails, spring elements are utilized. These spring elements simulate the mechanical behavior and interaction between the various components of the track system, providing an accurate representation of the overall system dynamics. A flexible dynamic model for the turnout is established using the modal superposition method, taking into account the variable cross-section of the steel rails, the utilization of shared baseplates among multiple rails, and the intricate and diverse constraint characteristics between the turnout steel rails. This modeling approach accurately captures the dynamic behavior and interactions of the components, enabling a comprehensive analysis of the turnout's response under various loading conditions. By considering the modal properties of the individual components, the model provides valuable insights into the performance and dynamic characteristics of the turnout, facilitating in-depth investigations and ensuring accurate predictions of its behavior.

In the resolution of dynamics problems within the wheel-rail contact system, the trajectory method is employed to compute the position and contact angle of the wheel-rail contact point, along with other pertinent geometric parameters. Subsequently, the Hertz non-linear elastic contact theory is utilized to determine the equivalent penetration depth, which is then used to calculate the normal vector of the wheel-rail contact. This approach ensures accurate determination of the contact behavior and provides essential information for further analysis of the dynamic response and performance of the wheel-rail system. A time-domain model for the rigid-flexible coupled dynamics of the high-speed vehicle-turnout system is established using the Kalker simplified theory and FASTSIM algorithm. This model calculates the relationships between the tangential force, creep force, and creepage ratio in the wheel-rail contact, as well as the wheel-rail creep forces. It considers the dynamic interactions between the vehicle and the turnout system, providing a comprehensive analysis of their dynamic behavior and performance under varying conditions.

2.2 Model verification

To ensure the accuracy of subsequent calculations, it is imperative to validate the vehicle-turnout coupled dynamic model. In this regard, a comparison is made between the calculated results of lateral wheel-rail forces, derailment coefficient, wheel load reduction, and vehicle body vibration acceleration during a sideways passage of the train at a speed of 160 km/h pass 42# turnout in the diverging route of the facing move and the corresponding results presented in reference [14]. The outcomes of this comparison are summarized in Table 1.

	The maximum derailment coefficient (switch rail side)	The maximum wheel unloading rate of switch rail (switch rail side)	The maximum wheelset lateral force (kN)	The maximum vertical vibration acceleration of the car body (m/s^2)	The maximum lateral vibration acceleration of car body (m/s^2)
Literature [14] Calculation results	0.57	0.26	27.93	0.03	0.69
Results of this model calculation	0.67	0.33	33.00	0.11	0.91

Table 1: Comparison of dynamic performance metrics

Based on the comparison presented in Table 1, the computed results of the model developed in this study consistently exhibit a slight overestimation compared to the calculations reported in reference [14]. This discrepancy can be attributed to the utilization of a distinct vehicle model and the incorporation of turnout flexibility in the current analysis. Nonetheless, the observed differences remain within an acceptable range, and the overall trends demonstrate a notable similarity, thereby affirming the reliability and validity of the proposed model.

3 Analysis of crucial influencing factors on stability of high-speed vehicles passing through turnouts in the diverging route

Drawing upon orthogonal tables and non-repetitive saturated factorial design methods, an $L_{21}\left(2^{11}\right)$ two-level factorial design was meticulously constructed to assess the pivotal factors that exert a substantial influence on the stability of pass turnouts in the diverging route. The design framework incorporates careful consideration of potential variables that may significantly affect the smooth and consistent movement when pass turnouts in the diverging route, thus facilitating a rigorous analysis of the prominent influencing factors associated with the observed stability.

3.1 Definition of factor levels

In order to discern the critical influencing factors that profoundly impact the stability of pass turnouts in the diverging route, a meticulous analysis is conducted on the factors that exert a substantial influence on the dynamic performance of the vehicle-turnout system. The objective is to quantify the significance and magnitude of influence attributed to each factor. This enables the prioritization and selection of the most significant factors, which play a pivotal role in determining the overall lateral stability of trains during switch crossings. Based on the research findings documented in reference [15], this study adopts an initial selection of eleven influencing factors for a rigorous two-level factorial analysis. These factors include turnout crossing speed, axle load, wheel-rail wear, wheel-rail friction coefficient, track irregularities, fastening system stiffness, and damping. The values for certain factors are explicitly

defined to ensure clarity and precision in the analysis. For example, the switch crossing speed is categorized into a normal level of 160 km/h (design speed), a low level of 120 km/h, and a high level of 200 km/h. On the other hand, for factors that are challenging to directly quantify, such as wheel and rail profile, two distinct analysis levels are established: a low level representing worn profiles and a high level representing unworn profiles. The definitions of different levels for the selected 11 analysis factors are presented in Table 2.

In Table 2, factors F to J correspond to the influence of geometric irregularities in the turnout area. The main focus of this study is to investigate the effects of horizontal, longitudinal, vertical, and gauge irregularities on the stability of train operations. In the specific context of this research, which pertains to the 42# high-speed turnout with maximum permissible speeds of 350 km/h in the through route and 160 km/h in the diverging route, the low-level definitions for factors F, G, H, and J are determined by utilizing time-domain samples of horizontal, longitudinal, vertical, and gauge irregularities generated from the prescribed spectrum of irregularities for China's high-speed ballasted track [16]. Furthermore, the different level definitions for factor E are established based on the distinct profiles observed in the combined design and measured worn rail at the critical section of the rail head, as depicted in Figure 1.

Numbered	Influencing factors	Level of influencing factors		
		Normal levels(0)	Low level(-1)	High level(1)
A	The speed of the train passing the turnout	160 km/h	120 km/h	200 km/h
B	Train axle	12 t	8 t	16 t
C	Wheel profile	/	See literature[17] Running 250,000 km LMA profile	LMA standard profile
D	Wheel-rail friction coefficient	0.3	0.1	0.5
E	Rail profile	/	Wear and tear	Standard profile of 42# high-speed turnout
F	Horizontal irregularities	/	Yes	No
G	Alignment irregularity	/	Yes	No
H	Vertical irregularity	/	Yes	No
J	Guage irregularity	/	Yes	No
K	Fastener stiffness	25 kN/mm	10 kN/mm	40 kN/mm
L	Fastener damping	45 kN·s/m	30 kN·s/m	60 kN·s/m

Table 2: Level types of analysis factors for influencing stability of high-speed vehicles passing through 42# turnout in the diverging route.

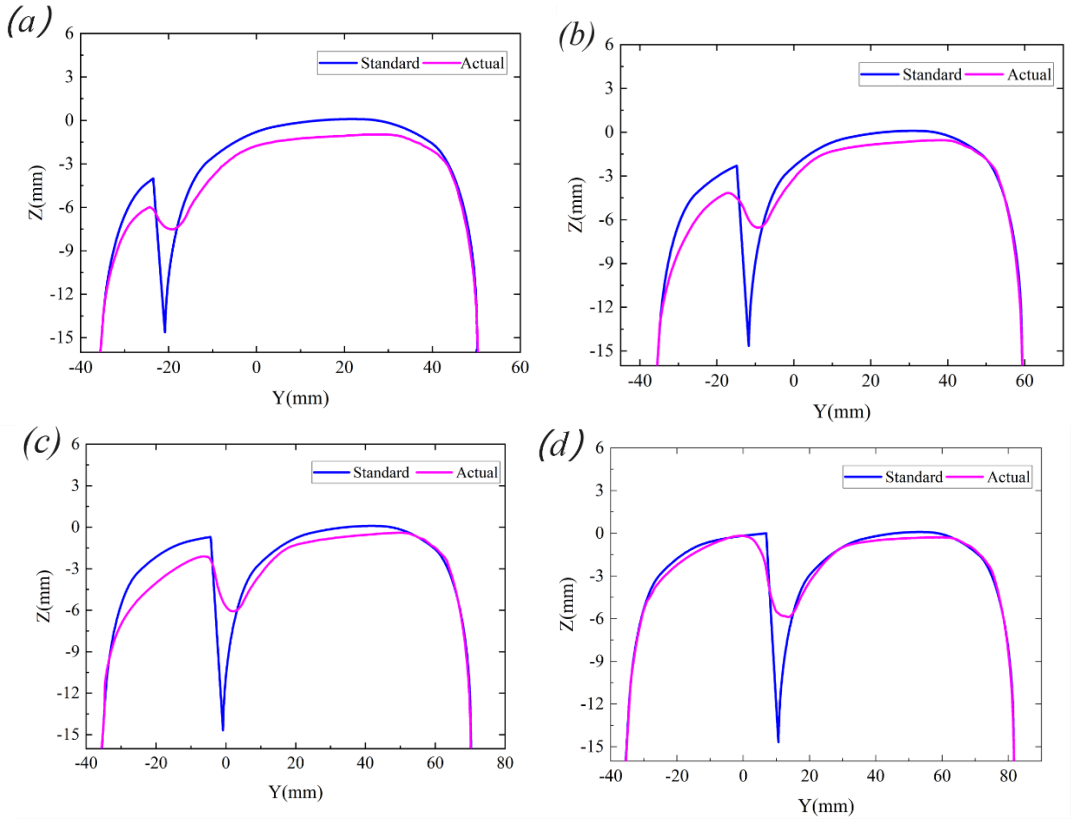

Figure 1: Different levels of definition of number E influencing factors; (a) switch rail with rail head width 15mm; (b) switch rail with rail head width 25mm; (c) switch rail with rail head width 35mm; (d) switch rail with rail head width 45mm

3.2 Non-replicated saturated experimental design scheme

After determining the analysis levels for factors influencing the stability of trains at turnouts, the subsequent step entails the identification of key indicators that exert a significant influence on the stability of train operations. In this study, a rigorous experimental design approach was adopted, employing the $L_{21}\left(2^{11}\right)$ non-replicated saturated factorial design method and orthogonal tables. This enabled the construction of twelve meticulously planned experimental runs, carefully considering the eleven selected influencing factors. The principal objective of these experimental runs was to estimate the effects of each factor on the overall stability. For a comprehensive understanding of the experimental design scheme, including precise details and the effects of each factor, please refer to Table 3.

Experiment	A	B	C	D	E	F	G	H	J	K	L
1	1	1	-1	1	-1	-1	-1	1	1	1	-1
2	-1	1	1	-1	1	-1	-1	-1	1	1	1
3	-1	1	1	1	-1	1	1	-1	1	-1	-1
4	1	1	1	-1	1	1	-1	1	-1	-1	-1
5	-1	-1	1	1	1	-1	1	1	-1	1	-1
6	-1	1	-1	-1	-1	1	1	1	-1	1	1
7	1	-1	1	-1	-1	-1	1	1	1	-1	1
8	1	-1	1	1	-1	1	-1	-1	-1	1	1
9	-1	-1	-1	-1	-1	-1	-1	-1	-1	-1	-1
10	-1	-1	-1	1	1	1	-1	1	1	-1	1
11	1	1	-1	1	1	-1	1	-1	-1	-1	1
12	1	-1	-1	-1	1	1	1	-1	1	1	-1

Table 3: Experimental design scheme for investigating factors affecting the stability

Based on the vehicle-turnout coupled dynamic model established in Section 1.1, a comprehensive analysis was conducted by subjecting the proposed experimental design schemes to rigorous simulation calculations under passing turnouts in the diverging route condition. The objective was to determine the dynamic responses of the wheel-rail system for each of the 12 schemes. To evaluate the stability of pass turnouts in the diverging route, key indicators, including the maximum values of wheel-rail lateral force, bogie lateral vibration acceleration, car body lateral vibration acceleration, and the Sperling stability index, were carefully selected as observed values within the statistical analysis framework. The evaluation results of these indicators, which play a vital role in assessing the train's lateral stability, are presented in a concise and scientifically rigorous manner in Table 4.

Experiment	Maximum wheel-rail later(kN)	Maximum bogie lateral vibration acceleration(m/s^2)	Maximum car body lateral vibration acceleration (m/s^2)	The lateral Sperling index
1	24.61	8.83	1.82	2.7239
2	54.57	2.42	0.63	1.5995
3	47.49	3.57	0.73	1.6429
4	94.39	3.88	2.24	2.5361
5	49.14	2.01	0.71	1.6456
6	27.70	3.73	0.74	1.8251
7	47.49	4.98	1.62	2.1346

8	93.96	8.15	1.51	2.1634
9	25.34	3.73	0.94	1.9153
10	8.06	3.04	0.80	1.6736
11	12.33	5.31	1.68	2.5996
12	24.18	3.90	1.22	1.9127

Table 4: Calculated kinetics of the observations

3.3 Significant Factor Selection

Utilizing the $L_{21}\left(2^{11}\right)$ saturated fractional factorial design method in this research, the primary objective is to discern the significant influencing factors. Once the necessary evaluation metrics are obtained, it becomes imperative to conduct further computations to ascertain the effects of the various factors. In accordance with the statistical model outlined in reference [15], the effects estimation of various influencing factors is obtained and presented in Table 5. Subsequently, a graphical analysis method is applied to discern the factors that exert a more pronounced impact on the stability of pass turnouts in the diverging route. The selection of these influential factors is based on a semi-normal probability distribution graph, as depicted in Figure 2.

Analysis factor	Wheel-rail lateral force	Bogie lateral vibration acceleration	Carbody lateral vibration acceleration	The lateral Sperling index
A	14.11	2.758	0.9233	0.6281
B	2.15	0.322	0.1733	0.2470
C	44.14	-0.589	0.0400	-0.1547
D	-6.35	1.378	-0.0233	0.0876
E	-3.99	-2.072	-0.0133	-0.0730
F	13.72	-0.168	-0.0267	-0.1441
G	-15.43	-1.092	-0.2067	-0.1419
H	-1.08	-0.102	0.2033	0.1176
J	-16.08	-0.012	-0.1667	-0.1663
K	6.51	0.755	-0.2300	-0.1053
L	-3.51	0.285	-0.1133	-0.0635

Table 5: Effect estimation of different impact factors

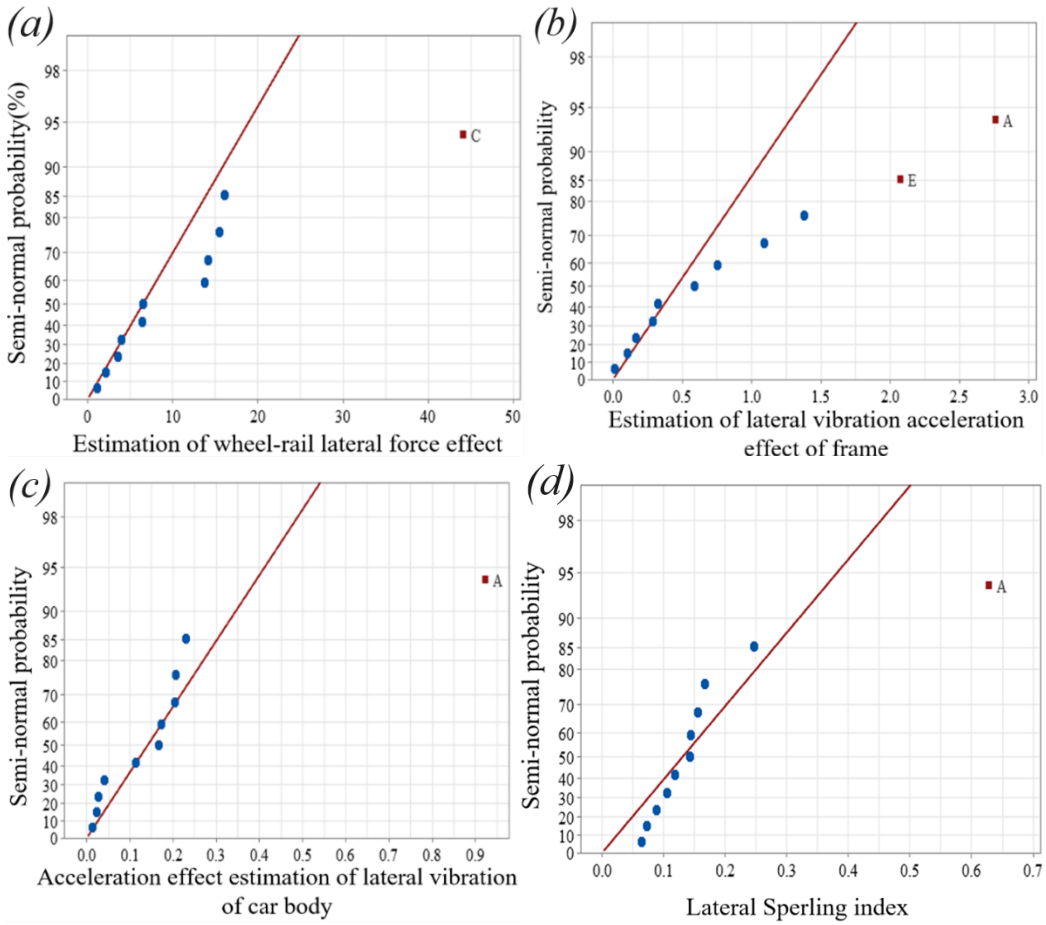

Figure 2: The semi-normal probability distribution diagram of significant impact factors is screened; (a) Semi-normal probability distribution diagram of wheel-rail lateral force effect; (b) Semi-normal probability distribution diagram of lateral vibration acceleration effect of frame; (c) Semi-normal probability distribution diagram of lateral vibration acceleration effect of car body; (d) Horizontal Sperling index effect semi- normal probability distribution diagram.

Based on the analysis of the semi-normal probability plots depicted in Figure 2, it is observed that each observed variable exhibits certain data points that deviate significantly from the reference line, denoted by the red dots. These deviations suggest the presence of notable influencing factors. Accordingly, the significant influencing factors for the lateral wheel-rail force are identified as factors C, while factors A and E emerge as significant influencing factors for the lateral bogie vibration acceleration. Additionally, factors A are also recognized as significant influencing factors for both the lateral body vibration acceleration and the lateral Sperling index. Among them,factor A corresponds to the train speed, factor C pertains to the wheel profile, and factor E represents the rail profile.

4 Impact of key factors on the stability of vehicles passing through turnout in the diverging route

The present investigation employs a Plackett-Burman non-replicated saturated fractional factorial design method, utilizing orthogonal arrays, to systematically discern the crucial factors that exert substantial influence on the observed values. The results demonstrate that train passing speed, wheel tread profile, and rail profile emerge as the primary determinants. Subsequently, a meticulously developed rigid-flexible coupled dynamic model is employed to scrutinize the inherent relationships between these three factors and their respective impacts on the stability of vehicle motion.

4.1 Impact of driving speed

Utilizing a vehicle-turnout rigid-flexible dynamic model, this scholarly investigation aims to conduct a comprehensive assessment of the dynamic performance of a vehicle passing through 42# turnout in the diverging route of the facing move under ideal conditions. The study systematically examines the influence of different crossing velocities, specifically 120 km/h, 140 km/h, 160 km/h, 180 km/h, and 200 km/h, on the vehicle's lateral reverse dynamic characteristics. Notably, the turnout region's unique structural configuration introduces irregularities in the profile of the swich rail side, resulting in a more pronounced dynamic response of the wheel-rail interaction compared to the straight rail side. Consequently, the primary focus of this study is to analyze and evaluate the dynamic response of the wheel-rail interaction specifically on the swich side.

The temporal profiles of the lateral forces acting on the switch side by the first wheel of the first bogie in the forward direction during the vehicles passing through 42# turnout in the diverging route at different velocities are graphically presented in Figure 3(a). The observed trends in the temporal variations of the lateral forces on the swich side exhibit consistency across the range of velocities considered. Within the switch area, significant lateral impacts occur as a result of wheel flange contact, with higher velocities yielding more pronounced impacts and higher peak values of lateral forces. In contrast, the lateral impacts within the frog area are comparatively negligible, and the influence of velocity on the lateral forces in this region is deemed negligible. Notably, when the velocity reaches 200 km/h, distinct fluctuations manifest in the lateral forces experienced at the wheel-rail interface along the guiging curve. This behavior can be attributed to the escalating centrifugal force resulting from the vehicle's traversal of the curve at higher velocities, thereby intensifying the wheel-rail interaction.

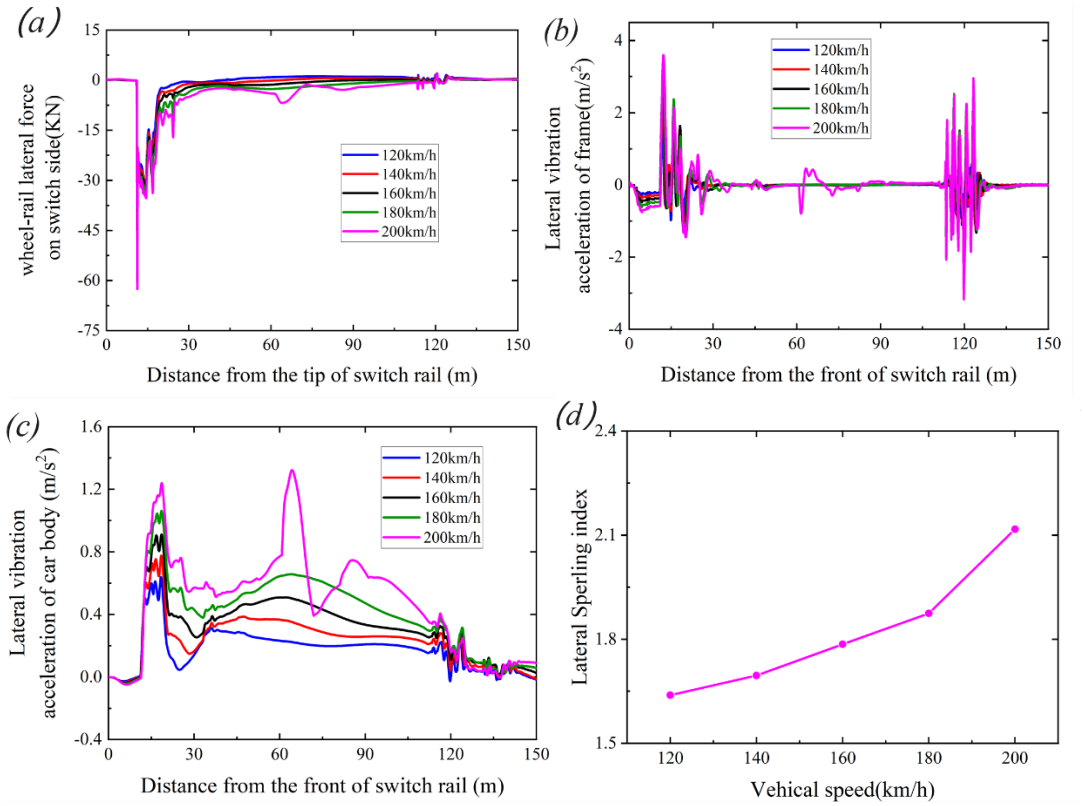

Figure 3: The influence of driving speed on the stability of vehicles passing through 42# turnout in the diverging route; (a) Wheel-rail lateral force; (b) Lateral vibration acceleration of frame; (c) Lateral vibration acceleration of carbody; (d) The variation of lateral Sperling index with velocity.

The lateral acceleration vibrations of the bogie and the vehicle passes turnout in the diverging route of the facing move at different velocities are analyzed. Figure 3(b) presents the temporal profiles of the lateral acceleration vibrations in the bogie, while Figure 3(c) illustrates the corresponding vibrations in the vehicle body. The findings reveal that as the vehicle's speed increases, both the bogie and vehicle body exhibit amplified magnitudes of lateral acceleration vibrations. However, the fundamental characteristics and variation patterns of these vibrations remain consistent within the examined velocity range, up to a maximum of 180 km/h. At a velocity of 200 km/h, distinct variations are observed in the temporal characteristics of the lateral acceleration vibrations for both the bogie and the vehicle body. The lateral acceleration vibrations of the bogie exhibit significant fluctuations not only in the switch and frog areas but also along the transition curve segment. Conversely, the lateral acceleration vibrations of the vehicle body display unique waveform patterns and a shift in the location of peak values compared to speeds below 180 km/h. The maximum lateral acceleration vibration of the vehicle body occurs at a position 64.24 m from the point of the swich rail, measuring 1.32 m/s². This behavior can be attributed to intensified wheel-rail interaction at that specific location, resulting in substantial modifications to the vehicle body's vibration response. Notably, at a speed of 120 km/h, the maximum lateral acceleration vibration of the vehicle body is 0.64

m/s², indicating a 29.67% reduction compared to a speed of 160 km/h. With the velocity increased to 200 km/h, the maximum lateral acceleration vibration of the vehicle body exhibits a 45.05% increase, reaching 1.32 m/s² in magnitude, relative to a speed of 160 km/h.

The Sperling stability index, derived from the analysis of vehicle lateral acceleration vibrations during pass turnouts in the diverging route, is graphically presented in Figure 3(d). The index demonstrates a positive correlation with increasing velocities. At a speed of 120 km/h, the lateral Sperling stability index measures 1.64, reflecting an 8.40% decrease compared to the permissible speed of 160 km/h. Conversely, at 200 km/h, the index rises to 2.12, indicating an 18.44% increase. These findings underscore the significant influence of speed on the vehicle's lateral stability during vehicles pass 42# turnout in the diverging route of the facing move. Higher speeds amplify the dynamic interaction between the wheel and rail, resulting in diminished stability. Consequently, adhering to the recommended speed limit during practical operations is advisable to maintain optimal stability.

4.2 Effect of wheel profile

This scholarly investigation examines the influence of different degrees of wheel wear on the lateral dynamic performance of trains during vehicles pass 42# high-speed turnout in the diverging route of the facing move through the switch zone . By employing a vehicle-turnout rigid-flexible dynamic model and considering standard LMA profiles from reference [17], as well as worn wheel profiles obtained at specific mileage intervals (50,000 km, 100,000 km, 150,000 km, 200,000 km, and 250,000 km), the study aims to analyze the impact of varying levels of wheel wear on the dynamic behaviors during vehicles pass turnouts in the diverging route.

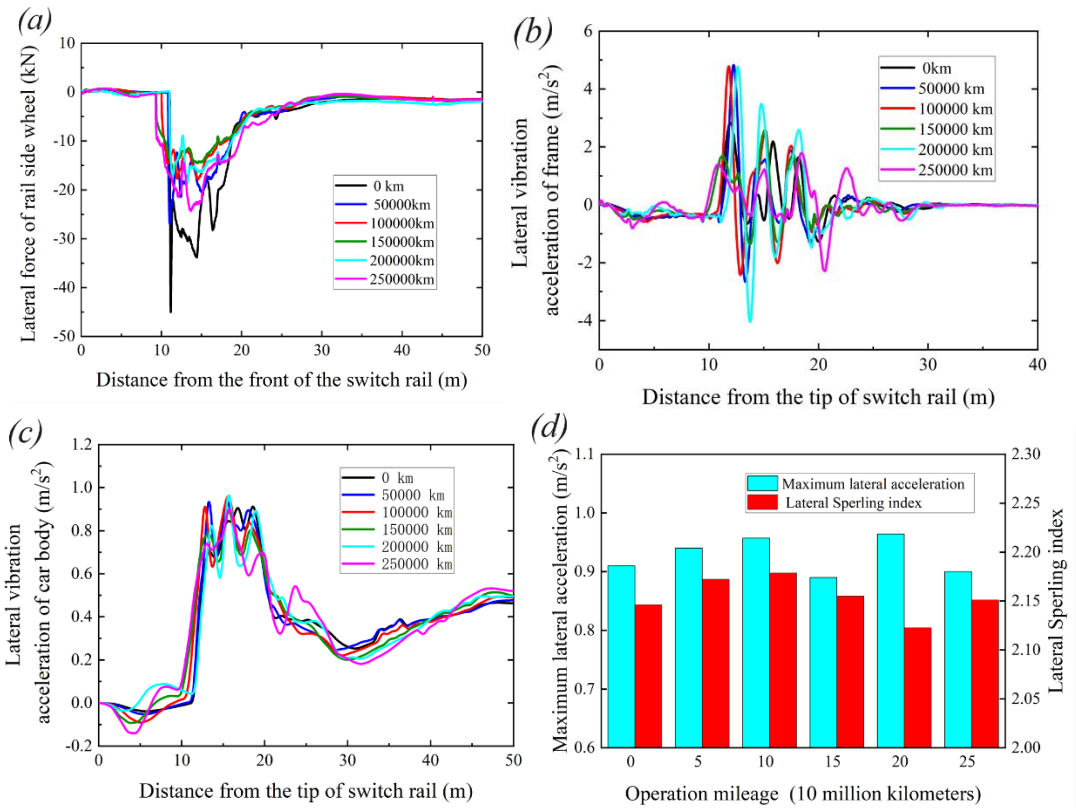

Figure 4: The influence of wheel profiles on the stability of vehicles passing through turnouts in the diverging route of the facing move; (a) Wheel-rail lateral force in switch side; (b) Lateral vibration acceleration of frame; (c) Lateral vibration acceleration of car body; (d) Lateral vibration acceleration of carbody and lateral Sperling index.

According to the data presented in Figure 4(a), the lateral wheel-rail forces on the point rail side exhibit a decreasing trend as the operational mileage increases up to 150,000 kilometers. At this mileage, the maximum lateral force reaches 15.74 kN, which is a reduction of 65% compared to the standard LMA wheel profile with a maximum lateral force of 45.04 kN. However, beyond 150,000 kilometers, the lateral forces start to increase. For instance, at an operational mileage of 250,000 kilometers, the maximum lateral force is 24.35 kN, indicating a reduction of 45.96% compared to the standard LMA wheel profile.

Furthermore, the vehicle's lateral vibration acceleration is significantly affected by the wheel profile. The peak acceleration values are observed to vary with the operational mileage. At an operational mileage of 50,000 kilometers, the peak acceleration reaches its maximum value of 4.83 m/s2, representing a 41.41% increase compared to the standard wheel profile. Conversely, at an operational mileage of 250,000 kilometers, the peak acceleration decreases to its minimum value of 2.29 m/s2, indicating a 19.01% reduction compared to the standard wheel profile

According to the findings presented in Figure 4(c), the maximum lateral vibration acceleration of the vehicle is observed to be minimal at an operational mileage of 150,000 kilometers, measuring 0.89 m/s2. Conversely, the highest value is recorded at an operational mileage of 200,000 kilometers, reaching 0.96 m/s2. These values correspond to a decrease of 2.20% and an increase of 5.49%, respectively, compared to the standard wheel profile.

On the other hand, Figure 4(d) illustrates the variation of the lateral Sperling stability index. It is noteworthy that the index exhibits its minimum value of 2.12 at an operational mileage of 200,000 kilometers, while the maximum value of 2.18 is observed at an operational mileage of 100,000 kilometers. These values indicate a decrease of 1.40% and an increase of 1.40%, respectively, in comparison to the standard wheel profile value of 2.15.

In summary, the influence of wheel wear on the wheel-rail lateral forces is pronounced, while its impact on the lateral vibration acceleration of the vehicle and the lateral Sperling stability index is relatively moderate.

4.3 Effect of rail profile

The rail profile in the switch and frog areas of 42# turnout was meticulously surveyed, and the findings are depicted in Figure 1. The analysis reveals notable indications of wear and tear on critical cross-sectional profiles of the swich rails, particularly when subjected to intricate operational conditions.

Analysis of Figures 5(a) and (b) demonstrates that the variation in rail profile during vehicles pass 42# turnout in the diverging route of the facing move has a substantial impact on the wheel-rail lateral forces.. This effect arises from the direct influence of rail profile changes on the wheel-rail contact characteristics, resulting in significant shifts in the contact point position. Comparing the worn rail profile to the standard profile, it is observed that the onset of wheel loading transition occurs earlier, while the termination position remains unaltered. As a consequence, the wheel loading transition segment is extended, and a marked discontinuity in the contact point position is observed after the transition.

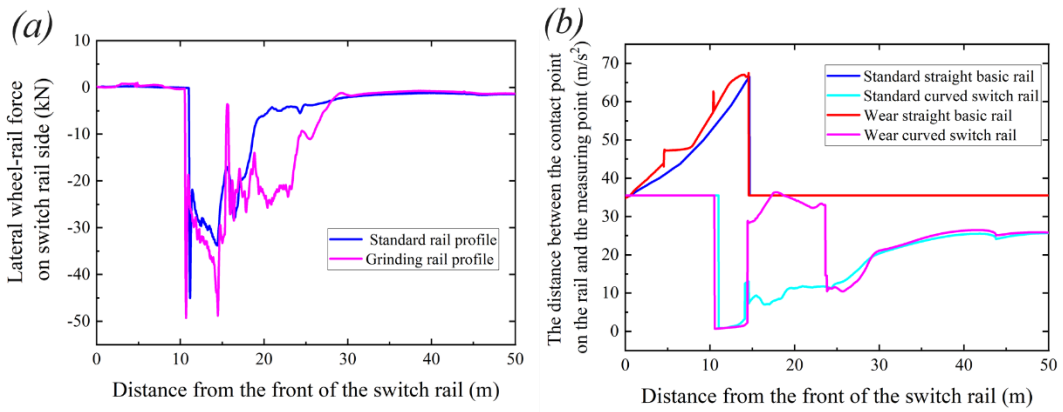

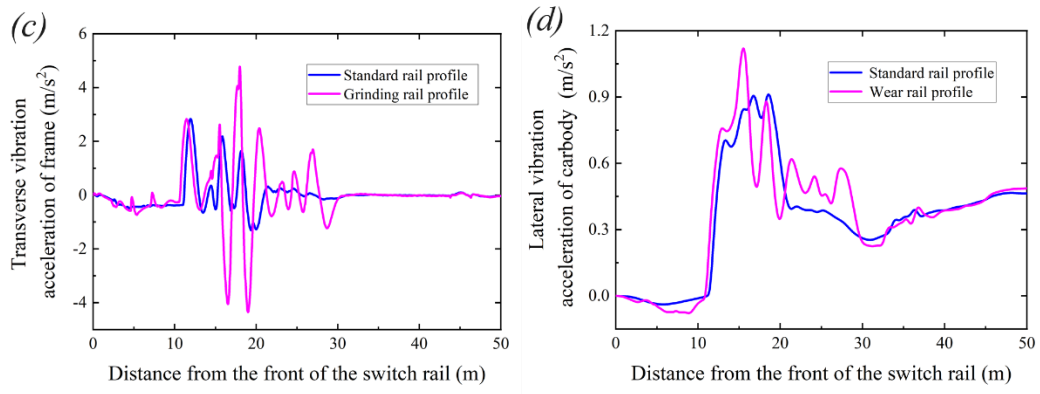

Figure5. The influence of rail profile on the stability of vehicle side reverse turnout; (a) Wheel-rail lateral force diagram; (b) Wheel-rail contact trace on switch rail side; (c) Transverse vibration acceleration of frame; (d) Lateral vibration acceleration of car body.

The findings from Figures 5(c) and (d) reveal a substantial increase in lateral vibration acceleration of the vehicle chassis following rail wear, surpassing the levels observed under standard rail profile conditions. Specifically, the maximum lateral vibration acceleration of the chassis exhibits a noteworthy augmentation of 69.36% relative to the standard profile. Conversely, the variation pattern of lateral vibration acceleration in the vehicle body displays alterations in response to mileage, resulting in relatively minor overall discrepancies, yet distinct changes in amplitude and oscillatory characteristics. Notably, the maximum lateral vibration acceleration of the vehicle body reaches 1.20 m/s², signifying a significant elevation of 31.87% compared to the standard profile. Furthermore, the derived lateral Sperling stability index registers a value of 2.32, representing a discernible increment of 7.44% over the standard profile. These empirical findings underscore the pronounced influence of rail profile on the vehicular ride stability.

5 Impact of key factors on the stability of vehicles passing through turnout in the diverging route

This paper is based on the vehicle side reverse over the turnout working conditions of each test design scheme simulation calculation, combined with graphical analysis method to screen out the influence of large-size of turnout area vehicle operation smoothness of the significant influence factor for the driving speed, wheel profile and rail profile, and carry out the traveling speed, wheel profile and rail profile on the turnout smoothness of the impact of the analysis, and get the following conclusions:

1. The results demonstrate a pronounced influence of train speed on various performance metrics, including wheel-rail lateral forces, frame vibration acceleration, lateral body vibration acceleration, and lateral Sperling index. These metrics exhibit a consistent positive correlation with increasing train speeds. Notably, at a speed of 120 km/h, the maximum lateral body vibration acceleration is observed to be 0.64 m/s², which reflects a significant decrease

of 29.67% compared to the value obtained at 160 km/h. In contrast, at a higher speed of 200 km/h, the maximum lateral body vibration acceleration reaches 1.32 m/s², indicating a substantial increase of 45.05% compared to the value recorded at 160 km/h. Consequently, it can be inferred that elevated train speeds have a discernible detrimental effect on the overall stability of the train system.

2. The whee profile demonstrates a substantial influence on wheel-rail lateral force and frame lateral vibration acceleration, while its effect on lateral body vibration acceleration and lateral Sperling smoothness index is comparatively minor. A comparison between the wheel tread profile and the standard profile reveals the most significant disparity in the maximum lateral body vibration acceleration after an accumulated operational distance of 200,000 kilometers, with a notable difference of 5.49%. Conversely, for an operational distance of 100,000 kilometers, the difference in the lateral Sperling smoothness index is relatively small, with a marginal variation of 1.40%. These findings emphasize the critical role of the wheel tprofile in governing lateral dynamics, particularly in terms of lateral forces and frame vibrations.

3. The rail profile exerts a significant influence on frame lateral vibration acceleration and lateral body vibration acceleration. In the case of worn rails, the maximum frame lateral vibration acceleration shows a substantial increase of 69.36% compared to the standard profile, while the maximum lateral body vibration acceleration exhibits a notable increase of 31.87%. These findings underscore the considerable impact of the rail profile on the overall stability of train operations, emphasizing the imperative of maintaining optimal rail profiles to ensure safe and reliable train performance.

Acknowledgements

The authors would like thank the support of the National Key R&D Program of China (2022YFB2603400), the Technology Research and Development Plan Program of China National Railway Group Limited (Grant No. K2022G034), the Sichuan Science and Technology Program of China (2023NSFSC0398, 2023NSFSC0884), the Fundamental Research Funds for the Central Universities (2682022ZTPY067).

References

[1] Polach O. Comparability of the non-linear and linearized stability assessment during railway vehicle design[J]. Vehicle System Dynamic, 2006, 44(sup1): 129-138.

[2] Wilson N, Huimin W, Tournay H, et al . Effects of Wheel/Rail Contact Patterns and Vehicle Parameters on Lateral Stability[J]. Vehicle System Dynamics, 2010, 48(sup1): 487-503.

[3] HE Xusheng, WU Huichao, GAO Feng.Test Study on Carbody Swing of High-Speed EMUs [J], Journal of Dalian JiaoTong Universty 2017, 38(01): 21-25.

[4] Chi Maoru, Zhang Weihua, Zeng Jin.etc. Influence of hunting motion on ride quality of railway vehicle [J]. Journal of Vibration Engineering, 2008, 21(06): 639-643.
[5] Sun Shanchao, Wang Weidong, LIU Jinchao.etc.Study of Carbody,s Serve Vibration Based on Stability Analysis of Vehicle System[J], China Railway Science, 2012, 33(02): 82-88.
[6] Yang Wenli. Analysis and Treatment of Track Irregularity Causing Swaying [J]. Modern Urban Rail Transit, 2008(05): 47-49.
[7] Zhang Zhichao, Li Gu, Du Ruitao.etc. Research on Transverse Vibration Problem for The Power Car of Power Concentrated EMU[J]. Railway Locomotive&Car, 2020, 40(03): 1-6+22.
[8] Cui Litong, Song Chunyuan, Li Xiaofeng.etc. Research on Abnormal Sloshing Problem of Railway Vehicles [J]. Automation Application, 2016(09): 140-142+145.
[9] Wang Shuguo, Si Daolin, Wang Meng.etc. Influence of Value Reduced for Switch Rail of High Speed Railway on Riding Quality[J]. China Railway Science, 2014, 35(03): 28-33.
[10] Jiang Jun, Wang Junping, Cui Rongyi. Research and Application of Influence Factors of Running Stationarity on High Speed Turnout [J]. China Railway, 2019(12): 84-90.
[11] Wang Ping, Ma Xiaochuan, Wang Jian, et al. Optimization of Rail Profiles to Improve Vehicle Running Stability in Switch Panel of High-speed Railway Turnouts[J]. Mathematical Problems in Engineering, 2017: 1-13.
[12] Wang Yonghua. Treatment Technologies of Track Irregularity in Turnout Area of Bengbu South Station of Beijing-Shanghai High Speed Railway [J]. Railway Engineering, 2022, 62(6): 45-48.
[13] Wanming Zhai. Vehicle-Track Coupled Dynamics [M].Science Press, 2020
[14] Cao Yang, Wang Ping, Deng Tao. Analysis on Cutting Mode Selection for Switch Blade Based on Wheel-rail System Dynamics[J]. Journal of The China Railway Society, 2014, 36(11): 73-79.
[15] Xu Jingmang. Research on Simulation of Curved Switch Rail Wear in High-Speed Turnout[D]. ChengDu: Southwest Jiaotong University, 2015.
[16] Wang Xuetong. Research on Fatigue Load Analysis and Life Prediction of High Speed Switch Rail[D]. ChengDu: Southwest Jiaotong University, 2021.
[17] Qian Yao, Wang Ping, Zhao Siqi, Xu Jingmang, Fang JiaSheng, Wang Shuguo.Influence of Wheel-rail Contact Geometry in High-speed Turnout Area[J]. Journal of The China Railway Society,2020,42(08):107-115.